



# Understanding Aerosol-Cloud-Radiation Interactions Using Local Meteorology and Cloud State Constraints

Alyson Douglas<sup>1</sup> and Tristan L'Ecuyer<sup>2</sup>

<sup>1</sup>University of Wisconsin-Madison

**Correspondence:** Alyson Douglas (ADouglas2@wisc.edu)

**Abstract.** While many studies have tried to quantify the sign and the magnitude of the warm cloud response to aerosol loading, both remain uncertain owing to the multitude of factors that modulate microphysical and thermodynamic processes within the cloud. Constraining aerosol-cloud interactions using the local meteorology and cloud liquid water may offer a way to account for covarying influences, potentially increasing our confidence in observational estimates of warm cloud indirect effects. Four years of collocated satellite observations from the NASA A-Train constellation, combined with reanalysis from MERRA-2, are used to partition warm clouds into regimes based on stability, the free atmospheric relative humidity, and liquid water path. Organizing the sizable number of satellite observations into regimes is shown to minimize the covariance between the environment or liquid water path and the indirect effect. Controlling for local meteorology and cloud state mitigates artificial signals and reveals substantial variance in both the sign and magnitude of the cloud radiative response, including regions where clouds become systematically darker with increased aerosol concentration in dry, unstable environments. The reverse Twomey effect, as it has been called, is evident even under the most stringent of constraints, confirming it is not an artificial signal or an isolated phenomenon. These results suggest it is not meaningful to report a single global sensitivity of cloud radiative effect to aerosol. To the contrary, we find the sensitivity can range from  $-0.46$  to  $0.11 \frac{Wm^{-2}}{\ln(AT)}$  regionally.

## 1 Introduction

Warm clouds play an important role in Earth's radiative balance, cooling the atmosphere and overring 25% of the Earth's surface on average and reflecting incoming shortwave radiation (Hahn and Warren, 2007). Perturbations in aerosol, whether from natural sources like sea spray or anthropogenic activities like industrial processing or biomass burning, lead to cloud-aerosol interactions that alter cloud radiative properties through two main effects, the albedo and the cloud lifetime effects. First identified by Twomey (1977), the albedo effect, or the first indirect effect as it's also known, suggests that clouds will become brighter as a result of aerosol loading. For a fixed liquid water path, increased aerosol within a cloud increases the number of cloud condensation nuclei (CCN), forcing the mean drop size to decrease which results in a brighter, more reflective cloud. The second indirect effect, or the cloud lifetime effect, proposed by Alrecht (1989) builds on this idea, noting that a decrease in mean drop size due to aerosol-cloud interactions may also delay the onset of collision coalescence, suppressing precipitation and, in turn, allowing the cloud to survive longer, grow larger, and ultimately reflect more shortwave radiation.



It has been estimated that including the cloud lifetime effect may increase the indirect effect by  $1.25\times$  compared to only quantifying the albedo effect (Penner et al., 2001).

However, observing the indirect effect is not as straight forward as looking out your window trying to spot brighter clouds. The magnitude and sign of the indirect effect is extremely sensitive to the method used to quantify it. As a result, the Inter-  
5 governmental Panel on Climate Change (IPCC) has low confidence in the current estimate of the global aerosol indirect effect (AIE) (Boucher et al., 2013). An accurate assessment of the total indirect effect will reduce error in climate sensitivity and further our understanding of the role of clouds in future climates (Bony and Dufresne, 2005).

Historically, methods of estimating the AIE employ a single linear regression of either the cloud's radiative effect or droplet radius against a proxy for aerosol concentration (Platnick and Twomey, 1994; Lohmann and Feichter, 2005). This method  
10 ignores all possible covariances between the cloud, aerosol, and any processes that may effect both and assumes one linear regression captures all effects, disregarding the effects of the local environment that can strongly modulate warm cloud properties and responses (Stevens and Feingold, 2009). Constraining the meteorology as well as cloud type can significantly alter the magnitude of the AIE compared to single, unconstrained global linear regression estimate (Gryspeerd et al., 2014). Regional analyses may capture the assorted responses and magnitudes, however these estimates still fail to extricate covariance with me-  
15 teorology. Observationally-based estimates simply cannot "turn off" the effects of entrainment or other environmental effects like a model, therefore analysis methods must prescribe a way to diminish the effect of these influences on cloud radiative effects.

Modeling provides one pathway for estimating the global AIE that explicitly accounts for local meteorological conditions, however low clouds are one of the largest sources of error in current global climate models (GCM) (Williams and Webb,  
20 2009). In particular, GCMs tend to overestimate liquid water path (LWP) in low clouds, which leads to an overestimation of the albedo (Nam et al., 2012). The artificially elevated LWP impacts the sensitivity to aerosol by assessing it under unrealistic conditions where the entrainment and precipitation are artificially dampened as a result of incorrect cloud parameterizations (Tsushima et al., 2016; Lee et al., 2009). Further, the microphysical processes of aerosol activation, nucleation, and eventual raindrop formation are only parameterized in current GCMs. The resolution is too coarse to emulate all scales of aerosol-  
25 cloud interactions hence the dependence on parameterizations and large uncertainty in model-derived estimates (Wood et al., 2016). Many cloud-aerosol processes are explicitly resolved in large eddy simulation (LES) models, but these are limited to small scales. A solution to this problem is a combination of global climate modeling guided by observation-based analysis and coordinated LES modeling to understand and quantify the AIE (Stephens, 2005).

Observation-based methods must, however, avoid the pitfalls of historical evaluations and define a clear methodology to limit  
30 covariance with local environmental conditions or buffering by the cloud. Cloud characteristics, such as LWP, can compound uncertainty in evaluating the AIE because the cloud state influences both radiative properties and susceptibility to aerosol (Lee et al., 2009; Feingold and Kreidenweis, 2002). The AIE is specifically defined as the cloud response to aerosol and the resulting effects on the radiative properties, and should not be conflated with impacts from the local meteorology or cloud morphology. When meteorology was accounted for, Gryspeerd et al. (2016) found the sensitivity of cloud fraction to aerosol loading was  
35 reduced by 80%. Quantifying the AIE therefore requires separating and constraining all processes that moderate cloud radiative



properties from those specifically due to aerosol-cloud radiation interactions (Stevens and Feingold, 2009). Organizing clouds into constrained, bounded spaces based on the external and internal covarying variables can improve aerosol-cloud-radiation impact estimates (Ghan et al., 2016).

This study examines the sensitivity of the radiative forcing of warm clouds to aerosol using a methodology that attempts to adequately constrain external influences while maintaining sufficiently robust statistics. Our methodology takes advantage of the vast sampling provided by satellites to systematically hold environmental conditions and cloud state approximately constant. We quantify the warm cloud sensitivity to aerosol for clouds of similar properties within similar environments. While satellite studies of aerosol-cloud interactions are by necessity correlative, the more covarying factors that are controlled (at the individual cloud level), the more closely we can approximate a causal relationship. In our study, a set of environmental conditions and cloud state parameters is referred to as a regime. This idea of stratifying observations into regimes has been successfully implemented before to analyze cloud processes (Williams and Webb, 2009; Chen et al., 2014; Oreopoulos et al., 2016).

The environmental and cloud state regimes adapted here are designed to homogenize the clouds and processes occurring, reducing covariance between aerosol interactions and other factors. Observationally-based, regime-dependent cloud processes have been discerned most often over large regional scales, however, divergent signals can be lost depending on the size of the region analyzed (Grandey and Stier, 2010). Even on small, local scales, variance in the meteorology alters the strength of the observed effects (Liu et al., 2016). A recent study using satellite observations with regime constraints, for example, found a definite relationship between the warm cloud AIE varies and atmospheric stability on a global scale (Chen et al., 2014).

LES of warm clouds have further shown that environmental instability can alter the effects of aerosol loading on warm clouds (Lee et al., 2012). The need to incorporate stability into AIE estimates has also been noted in prior observational studies (Sorooshian et al., 2009; L'Ecuyer et al., 2009; Su et al., 2010). Warm clouds in stable environments may show an increasing LWP with respect to aerosol loading while unstable environments may exhibit a decrease in LWP (Chen et al., 2014). Su et al. (2010) found the stability and rate of subsidence work to modulate aerosol-cloud-radiation interactions in warm clouds.

The effects of large scale subsidence and entrainment can be captured by the relative humidity (RH) in the free atmosphere which has been shown to exert a powerful influence on warm cloud characteristics (Wood and Bretherton, 2004). Entrainment of free atmospheric air drives the decoupling process. Thus including RH in aerosol sensitivity studies accounts for any possible influences of decoupling. Decoupling can lead to a cloud layer like marine stratocumulus to break up into cumulus, which form beneath the stratocumulus deck as it decouples. Models affirm the effects of entrainment on the cloud layer depend on RH as LES have shown RH moderates cloud feedbacks in low warm cloud simulations (Van der Dussen et al., 2015). Ackerman et al. (2004) and Bretherton et al. (2007) further demonstrated using an LES model that entrainment of dry air from the free atmosphere alters the distribution of liquid water within a cloud, which could modify aerosol-cloud interactions.

In his original work, Twomey postulated that cloud albedo ought to increase with aerosol provided LWP is held fixed; albedo is, to a first order, dependent on the LWP and effective radius. The LWP has been shown to clearly control the second AIE via its influence on precipitation suppression, therefore it can be inferred that LWP may be intrinsically tied to the magnitude of the AIE (L'Ecuyer et al., 2009; Sorooshian et al., 2009). Field campaign observations have confirmed this, for example during



the AMF-Azores campaign where the cloud response depended largely on the LWP (Liu et al., 2016). Failing to distinguish scenes by this important cloud state parameter could also lead to large covariance and/or buffering in the system by the LWP.

For these reasons, we adopt the relative humidity of the free atmosphere and boundary layer stability in conjunction with LWP to segment observations into regimes at the scale of individual satellite pixels. To illustrate the impact of these specific buffering factors, we sequentially investigate how observational estimates of the sensitivity of cloud to aerosol changes under increasing constraints. First, the sensitivity is constrained by only LWP to demonstrate the importance of accounting for cloud state alone when estimating aerosol response. Next, environmental regimes of stability and relative humidity are used segment warm clouds and, within each regime, the sensitivity of the cloud radiative effect to aerosol is assessed. These results are then further separated into LWP regimes to control for cloud state and environment simultaneously. Finally, the warm cloud sensitivity with regime constraints is derived on a regional basis to account for local influences not captured by the global regime partitions.

## 2 Methods

### 2.1 Data

The effect of aerosol on radiative properties is diagnosed from observations collected by the NASA A-Train constellation from 2007 to 2010. The A-Train is a series of synchronized satellites which allow for collocated observations from a variety of instruments (L'Ecuyer and Jiang, 2011). Environmental information is provided by collocated reanalysis data from the Modern-Era Retrospective analysis for Research and Applications Version 2 (MERRA-2). Collocated observations from multiple instruments, combined with high resolution reanalysis at the pixel scale, allows an unprecedented glimpse into the roles of the environment and cloud state in modulating cloud sensitivity to aerosol concentration.

### 2.2 Cloud

The Cloud Profiling Radar (CPR) on CloudSat and the lidar on Cloud-Aerosol Lidar and Infrared Pathfinder Satellite (CALIPSO) are used to restrict analysis to single layer warm clouds. The CloudSat 2B-CldClass-Lidar product that classifies cloudy pixels based on their vertical structure from merged radar and lidar observations is leveraged to filter out ice phase and multilayered cloud systems (Sassen et al., 2008; Austin et al., 2009). The Advanced Microwave Scanning Radiometer - Earth Observing System (AMSR-E) liquid water path (LWP) aboard the Aqua satellite is then used to limit observations to scenes where the LWP is above  $20 \frac{\text{g}}{\text{m}^2}$  and below  $400 \frac{\text{g}}{\text{m}^2}$  (Wentz and Meissner, 2007). Very thin clouds below  $20 \frac{\text{g}}{\text{m}^2}$  are likely thin veil clouds with low albedos that are not the focus of this analysis (Wood et al., 2018). An along satellite track cloud fraction is determined by finding the average number of warm cloud pixels that satisfy these criteria (seen by CloudSat or CALIPSO, below freezing level, and LWP greater than  $20 \frac{\text{g}}{\text{m}^2}$ ) over each 12 km segment of the CloudSat track, a scale that represents both the local scale length of the boundary layer and field-of-view used to define cloud radiative effects from Clouds and the Earth's Radiant Energy System (CERES) (Oke, 2002).



The cloud radiative effect is found by combining this along track warm cloud fraction with top of atmosphere (TOA) radiative fluxes from CERES. CERES has a total (.4 - 200  $\mu\text{m}$ ) and shortwave channel (0.4 - 4.5  $\mu\text{m}$ ) that allow outgoing shortwave and longwave fluxes at the top of the atmosphere to be estimated using appropriate bi-directional reflectance models. The shortwave cloud radiative effect (CRE) is then defined in terms of the all sky and inferred clear sky forcings from CERES and cloud fraction from CloudSat. Writing the all-sky net SW radiation at the top of the atmosphere as:

$$(F_{\text{SW}}^{\downarrow} - F_{\text{SW}}^{\uparrow})_{\text{All Sky}} = (F_{\text{SW}}^{\downarrow} - F_{\text{SW}}^{\uparrow})_{\text{Clear Sky}} \times (1 - \text{CF}) + (F_{\text{SW}}^{\downarrow} - F_{\text{SW}}^{\uparrow})_{\text{Cloudy}} \times \text{CF}$$

It is easy to show that:

$$F_{\text{All Sky}}^{\uparrow} - F_{\text{Clear Sky}}^{\uparrow} \times (1 - \text{CF}) = \text{CRE}$$

where  $\text{CRE}_{\text{SW}} = \text{CF} \times F_{\text{Cloudy}}^{\uparrow}$

The clear sky flux ( $F_{\text{Clear Sky}}^{\uparrow}$ ) is a regional, monthly mean estimate of cloud free outgoing shortwave radiation. The instantaneous CRE for each warm cloud observation is used in conjunction with aerosol information and corresponding instantaneous cloud state and meteorological state constraints to derive the sensitivity of the cloud radiative effect to aerosol loading.

### 2.3 Aerosol

Aerosol index (AI) is used to characterize the concentration of aerosol. AI is the product of the Angstrom exponent and AOD at 550 nm both of which are derived from the Moderate-Resolution Imaging Spectroradiometer (MODIS) aboard the Aqua satellite. The Angstrom exponent, a measure of the turbidity of the atmosphere, is derived from multiple estimates of aerosol optical depth (AOD) at 550, 865, and 2100 nm (Ångström, 1929; Remer et al., 2005). The MODIS Angstrom exponent provides information about the size of the observed aerosol as well as concentration (Levy et al., 2010). Although AI is not a direct measurement of CCN in the air, it has a higher correlation with CCN compared to the AOD and is therefore more suitable for aerosol-cloud interaction studies (Stier, 2016; Dagan et al., 2017).

### 2.4 Sensitivity

The cloud sensitivity to aerosol, or  $\lambda$ , is defined here as the linear regression of the shortwave CRE against  $\ln(\text{AI})$ . The natural log of AI is used to better represent the effects of the smallest particles, which are more likely to act as CCN within a cloud (Köhler, 1936). The sensitivity is evaluated within environmental and cloud state regime frameworks on both global and regional scales. Variation in  $\lambda$  between regimes may signal buffering by the environment or cloud state. Throughout the study, although environmental and cloud state impacts are constrained through regimes, it cannot be stated with certainty that the observed changes in CRE are due to aerosol, only correlated with aerosol.

The unconstrained sensitivity or the sensitivity of cloud radiative effect to  $\ln(\text{AI})$  in the absence of constraints is computed as:

$$\lambda_0 = -\frac{\partial \text{CRE}}{\partial \ln(\text{AI})} \quad (1)$$



The partial derivative in this equation immediately implies influencing factors other than aerosols should be held fixed. Here this is accomplished by evaluating the sensitivity with increasing constraints on the partial differential through regimes.

To hold the cloud state fixed, the sensitivity is found for distinct LWP regimes and summed to yield a mean sensitivity:

$$\lambda_{LWP} = \sum_{k=1}^7 \left( - \frac{\partial \text{CRE}}{\partial \ln(\text{AI})} \right)_k N_k \quad (2)$$

- 5 Where  $N_k$  is the fraction of clouds that fall into LWP state  $k$ . Similarly, the sensitivity within environmental regimes, defined by the estimated inversion strength and relative humidity of the free atmosphere, can be computed, weighted, and summed to account for meteorological covariability:

$$\lambda_{ENV} = \sum_{j=1}^{10} \sum_{i=1}^{10} \left( - \frac{\partial \text{CRE}}{\partial \ln(\text{AI})} \right)_{i,j} N_{i,j} \quad (3)$$

By extension, both cloud and environmental conditions can be controlled via:

$$10 \quad \lambda_{BOTH} = \sum_{k=1}^7 \sum_{j=1}^{10} \sum_{i=1}^{10} \left( - \frac{\partial \text{CRE}}{\partial \ln(\text{AI})} \right)_{i,j,k} N_{i,j,k} \quad (4)$$

Finally, it is recognized that these bulk constraints do not fully capture all of the local factors that influence aerosol-cloud interactions. AI alone does not fully constrain the effect of aerosol composition which varies regionally. Thus, to control for these unaccounted for local effects, the sensitivity is further constrained by finding Eqn (4) on a  $15^\circ$  by  $15^\circ$  scale.

$$\lambda_{ALL} = \sum_{l=1}^{152} \sum_{k=1}^4 \sum_{j=1}^5 \sum_{i=1}^5 \left( - \frac{\partial \text{CRE}}{\partial \ln(\text{AI})} \right)_{i,j,k,l} N_{i,j,k,l} \quad (5)$$

## 15 2.5 Environmental Regimes

MERRA-2 reanalyses collocated with each CloudSat footprint is used to define local thermodynamic conditions that distinguish environmental regimes. The environmental regimes employed here provide a crude representation of the effects of the local meteorology acting on the cloud to inhibit or invigorate aerosol-cloud-radiation interactions. While these states, defined from percentile bins of the estimated inversion strength (EIS) and relative humidity at 700 mb (RH), do not capture the complete  
 20 range of environmental factors that influence warm cloud development, they have been shown to provide fairly robust bulk



classification for sorting satellite observations into meteorological regimes (Sorooshian et al., 2009; L'Ecuyer et al., 2009; Chen et al., 2014). Here, EIS is calculated using MERRA-2 temperature and relative humidity profiles. EIS incorporates effects of water vapor on the lower tropospheric static stability and is better correlated for all cloud types with cloud fraction (Wood and Bretherton, 2006). The relative humidity at 700 mb is used as a measure of the effect of entraining free tropospheric air. All observations within the 5% - 95% percentiles of both EIS and RH are partitioned into regimes. Environmental regime limits are defined such that there are the same number observations within each percentile of either EIS or RH. The regime bounds depend on the resolution used, which is varied to establish the degree to which environmental factors must be constrained to accurately characterize sensitivity.

## 2.6 Cloud Regimes

AMSR-E liquid water path, derived from the 19, 23, 37 GHz channels, is used to separate observations into cloud regimes (Wentz and Meissner, 2007). AMSR-E LWP is most accurate for low, marine warm clouds (Greenwald et al., 2007; Juárez et al., 2009). 99% of observations fell below a LWP of  $400 \frac{\text{g}}{\text{m}^2}$  and analysis was restricted to observations with LWP below this limit. Since CRE is proportional to the optical depth of a cloud, which is directly related to the LWP, the sensitivity has a strong covariance with LWP (Stephens, 1978; Lee et al., 2009; Wood, 2012). Holding LWP effectively constant is therefore essential to estimating the AIE (Lohmann and Lesins, 2002). The lowest LWP regimes have the least chance of precipitating; the sensitivities of these regimes are unlikely to be affected by secondary aerosol-cloud-precipitation effects.

## 3 Results

### 3.1 Unconstrained Sensitivity

The global sensitivity of warm cloud SW forcing to aerosol without any constraints, described by Equation (1), is  $-12.81 \frac{\text{Wm}^{-2}}{\ln(\text{AI})}$  (Figure 1). This seems to capture the AIE, after all the shortwave CRE increases with aerosol loading as expected. However, this unconstrained estimate ignores the roles of buffering and covariance. The indicated variation of SW CRE within each  $\ln(\text{AI})$  (red bars) bin alludes to variation in the overall effect not captured by a single linear regression. Although the  $R^2$  is high, without constraints, the increase in shortwave CRE cannot be attributed to only aerosol. Furthermore, from this estimate, no information is made known on how the sensitivity varies regionally, how cloud processes affect the AIE, or whether particular cloud states may be influenced more strongly by aerosol than others.

### 3.2 Sensitivity to Cloud State

The original description of the albedo effect by Twomey (1977) specified holding the LWP of the cloud constant. Following Twomey's original hypothesis, when warm clouds are separated into LWP regimes, it is clear that cloud morphology plays a role in modulating the magnitude of the sensitivity (Figure 2). The total weighted, summed sensitivity is  $-13.12 \frac{\text{Wm}^{-2}}{\ln(\text{AI})}$ . Low LWP clouds are less sensitive to aerosol. The sensitivity increases with LWP, peaking for cloud LWPs between .1 and .15



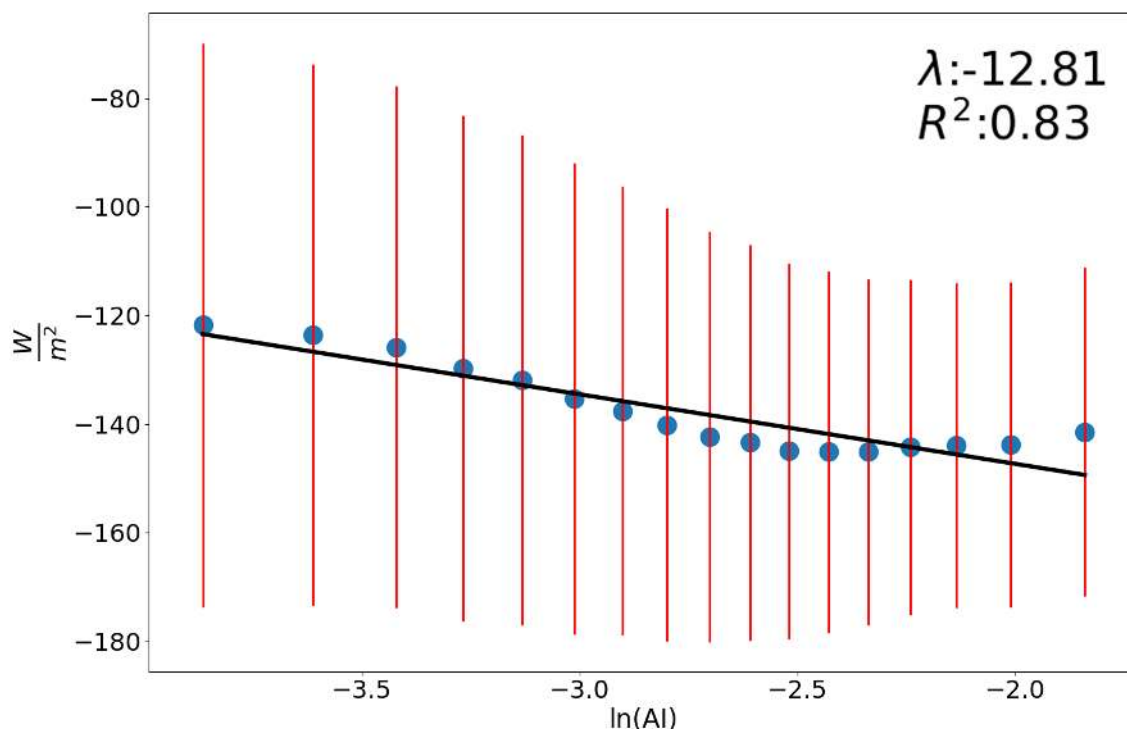
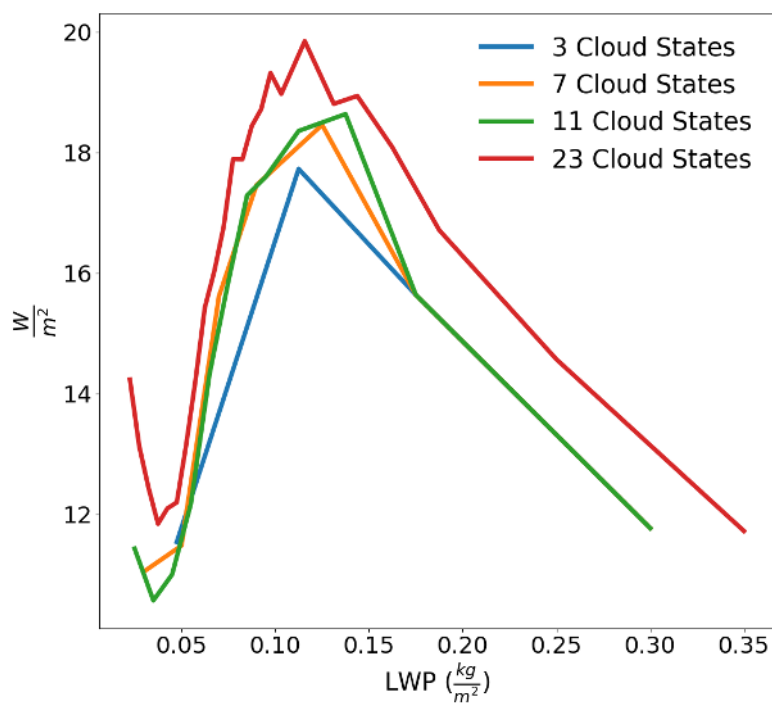


**Figure 1.** The sensitivity of CRE to aerosol ( $\lambda$ ) from equation (1) found globally without constraints on the environment, cloud state, or region.

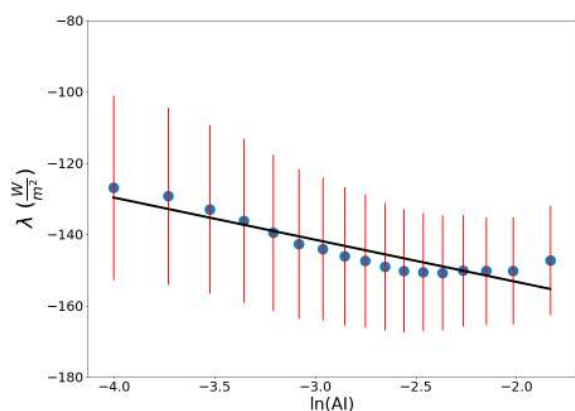
$\frac{kg}{m^2}$ . Beyond  $.15 \frac{kg}{m^2}$ , the trend reverses and the sensitivity decreases with LWP, consistent with the fact that thicker clouds are already bright and less susceptible to aerosol-induced changes (Fan et al., 2016). The non-linear relationship along with the known covariance between LWP and the AIE make it a vital component of the regime framework proposed here (Feingold, 2003). Constraints on LWP limit these influences.

- 5 The key to implementing appropriately stringent regime constraints is to determine the minimum number of cloud regimes required to adequately capture this LWP modulation of the total sensitivity. Observations were divided into 3, 7, 11, and 23 cloud regimes based on LWP. Overall,  $\lambda$  exhibits a similar trend regardless of resolution (the number of regimes used). The peak sensitivity for all partitions is around  $.1 \frac{kg}{m^2}$ , but using 11 or 23 regimes demonstrates the peak is actually closer to  $.15 \frac{kg}{m^2}$ . The amplitude of the sensitivity variation with LWP and the behavior at larger LWP is not well captured using only 4 LWP
- 10 bins. The use of 8 cloud regimes, on the other hand, generally reproduces the shape of the higher resolution bins but guarantees a large number of samples within each cloud regime appropriate for a linear regression, especially when later partitioning by additional influences.

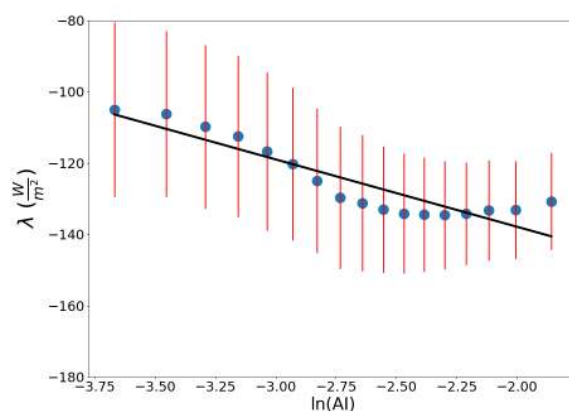




(a)



(b)



(c)

**Figure 2.** Values of the sensitivity of CRE to aerosol ( $\lambda$ ) from equation (2) for different resolutions of cloud state regimes. Weighted, summed  $\lambda_{LWP}$  is  $-13.12 \frac{Wm^{-2}}{\ln(AI)}$ . Plots of  $\ln(AI)$  against CRE below for LWPs between .04 to .06 (b) and .1 to .15 (c)  $\frac{kg}{m^2}$ .

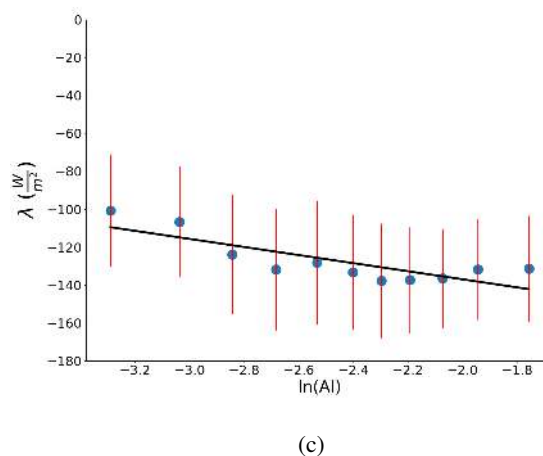
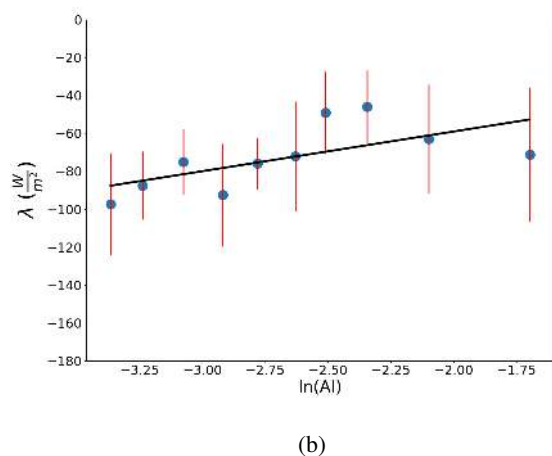
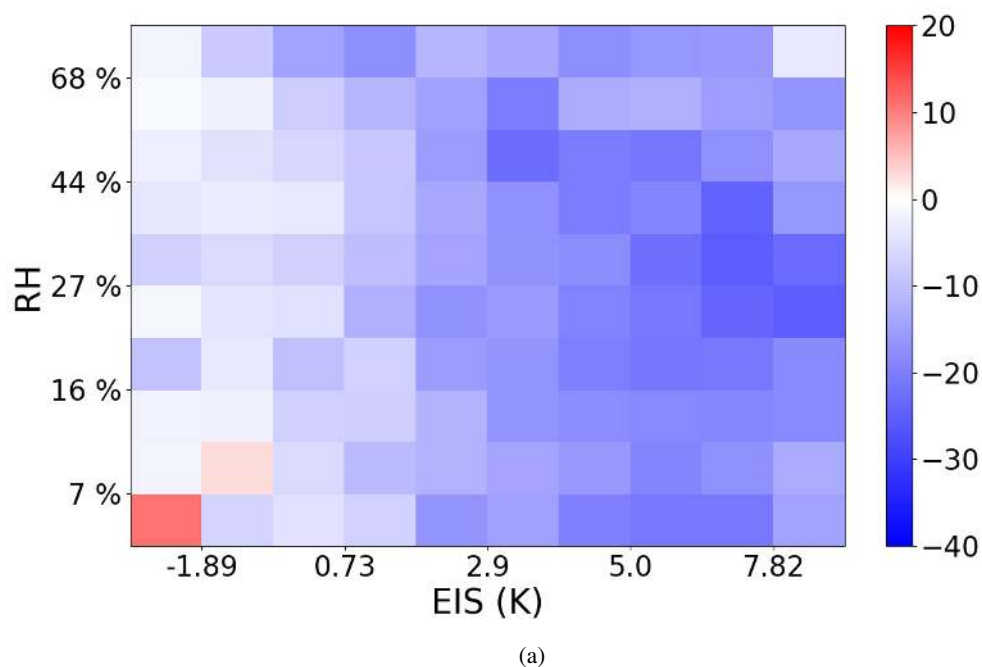


**Figure 3.** The sensitivity of CRE to aerosol ( $\lambda$ ) from equation (3) evaluated with constraints on the environment ( $-11. \frac{\text{Wm}^{-2}}{\ln(AI)}$ ). Plots of the individual regimes from an unstable, dry environment (b) and stable, moist environment (c).

### 3.3 Sensitivity within Environmental Regimes

Even when separated into cloud states, aerosol impacts on warm clouds can be strongly modulated by the local environment. To account for the local meteorology, warm clouds are separated into 100 environmental regimes defined according to the local



stability and free tropospheric humidity at the time they were observed (Figure 3). Within each EIS and RH regime, CERES shortwave CRE is linearly regressed against  $\ln(AI)$ . As the regime changes, the processes behind the cloud's response and resulting radiative sensitivity also change. The highest sensitivity is observed in stable regimes ( $EIS > 5.0$ ) with a moderately dry free atmosphere. In general, less stable regimes exhibit lower sensitivities for all RH. In the least stable and driest regimes, the sign of  $\lambda$  reverses, indicating that clouds become darker with increased aerosol loading, counter to the conventional view that polluted clouds become brighter and cool more effectively. The moisture content of free atmosphere appears to influence the sensitivities in stable regimes more than unstable regimes with a clear divide at  $EIS = 1$  K. Above 1 K,  $\lambda$  increases with increasing RH, while in less stable environments, RH plays only a secondary role in modulating the sensitivity. The most sensitive warm clouds reside in environments with a moderately dry relative humidity of around 27% for an extended range of stabilities from 5 to 10 K. Warming effects (positive sensitivities) as opposed to cooling effects, are observed in low stability, low humidity environments. A warming, or reverse Twomey, effect has been noted to occur in some regimes by others investigating the AIE (Chen et al., 2012, 2014). Consistent with these results, Christensen and Stephens (2011) found that up to 1/3 of ship-tracks, occurring in primarily low stability regions, are darker than their surroundings owing to their thermodynamic feedbacks. Accounting for this strong environmental modulation of sensitivity, the weighted global sensitivity calculated using Equation (3) is  $-11.04 \frac{Wm^{-2}}{\ln(AI)}$  (Figure 3).

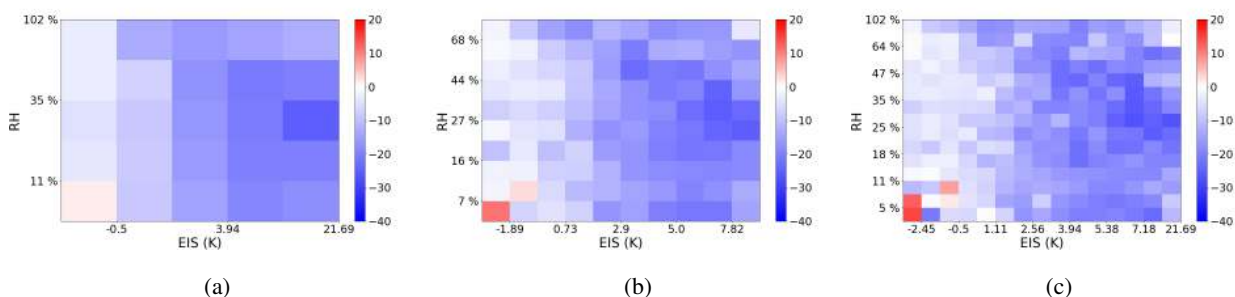


**Figure 4.** Sensitivity found within environmental frameworks of a) 25 ( $-11.29 \frac{Wm^{-2}}{\ln(AI)}$ ), b) 100 ( $-11.04 \frac{Wm^{-2}}{\ln(AI)}$ ) and c) 225 ( $-10.99 \frac{Wm^{-2}}{\ln(AI)}$ ) regimes of EIS and RH.

Again, for the partial derivative in Eqn (3) to be applied correctly, the number of partitions must be narrow enough to separate the various degrees of buffering by the local meteorology and yet allow an ample number of observations per environmental regime. To determine an optimal resolution for this dataset, the distribution of observations and sensitivity are separated into 5, 10, and 15 EIS and RH partitions representing 25, 100, and 225 environmental states respectively (Figures 4, 5). The distribution of observations among environmental regimes varies smoothly with resolution (Figure 5). The minimum number of samples decreases from 35532 to 2707 to 757 when the resolution increases from 25 regimes to 100 regimes to 225 regimes, respectively. The driest, most unstable and the moistest, stablest environmental regimes always have the largest number of observations.

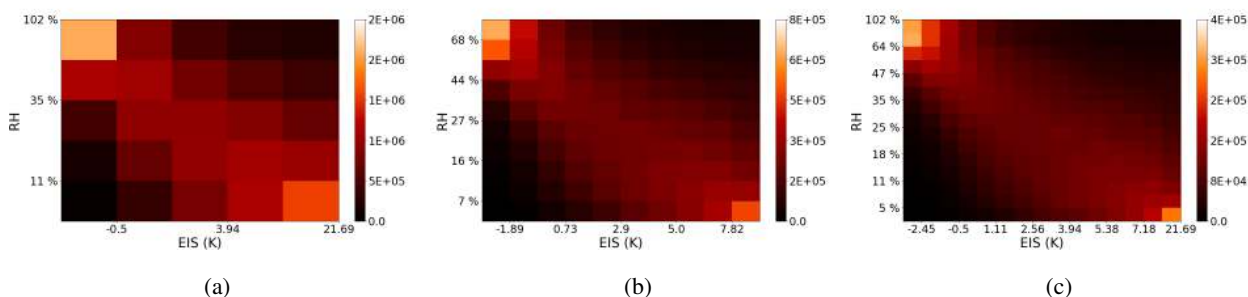


**Figure 5.** Frequency of clouds within environmental frameworks of a) 5, b) 10, and c) 15 regimes of both EIS and RH.

The total sensitivity decreases as the resolution increases, from  $-11.29$  to  $-11.04$  to  $-10.99 \frac{W_m^{-2}}{\ln(AI)}$  (Figure 4). The 5 by 5 framework degrades the smoothness in  $\lambda$  with respect to the different environmental states. The difference between the 10 by 10 and 15 by 15 estimates of sensitivity indicate that an increase in resolution after 10 partitions will lead to very little change in the overall sensitivity. However, an increased resolution decreases the number of clouds in all environmental regimes, which will be vital when the environmental regimes are further distributed among cloud states. The use of 100 regimes in analysis is appropriate to ensure proper distribution among all cloud states.

### 3.4 Accounting for Cloud and Environmental States

The preceding sections clearly demonstrate the importance of controlling for meteorological and cloud state dependencies when evaluating the sensitivity of cloud radiative effects to aerosol. To account for the covarying impacts of cloud state, the environment, and aerosols on cloud radiative effects, we must simultaneously control for each of these factors. Here we define three-dimensional regimes that hold LWP approximately constant while also constraining the local meteorology (Figure 6). The sensitivities estimated for each of the 700 resulting regimes are shown in Figure 6. The lowest LWP cloud regimes show a comparatively damped maximum sensitivity than the thicker cloud regimes. Higher LWP clouds exhibit an increasing maximum  $\lambda$ . The variation in magnitude between cloud regimes within the same environmental regimes confirms that LWP exerts a strong control in modulating the magnitude of the response and must be held constant when estimating the AIE. Mixing different cloud states in Figure 3 likely conflates differing signals, inaccurately representing the sensitivity in the most populous environmental regimes.

Again the constrained sensitivities show distinct evidence of an inverse Twomey effect where thin clouds in the driest, most unstable environments exhibit a warming, or darkening, response to aerosol loading. Within the environmental regimes that exhibit a darkening effect, the magnitude is strongly modulated by LWP, suggesting both the expected (cooling) and opposite (warming) responses depend on LWP, RH, and EIS. As LWP increases, a warming  $\lambda$  favors increasingly moist, stable environments. The maximum sensitivity is always observed in stable environments, but thin clouds, or low LWP cloud regimes, are more responsive to dry or moist free atmospheres. In thinner clouds, especially, aerosol loading will increase the number

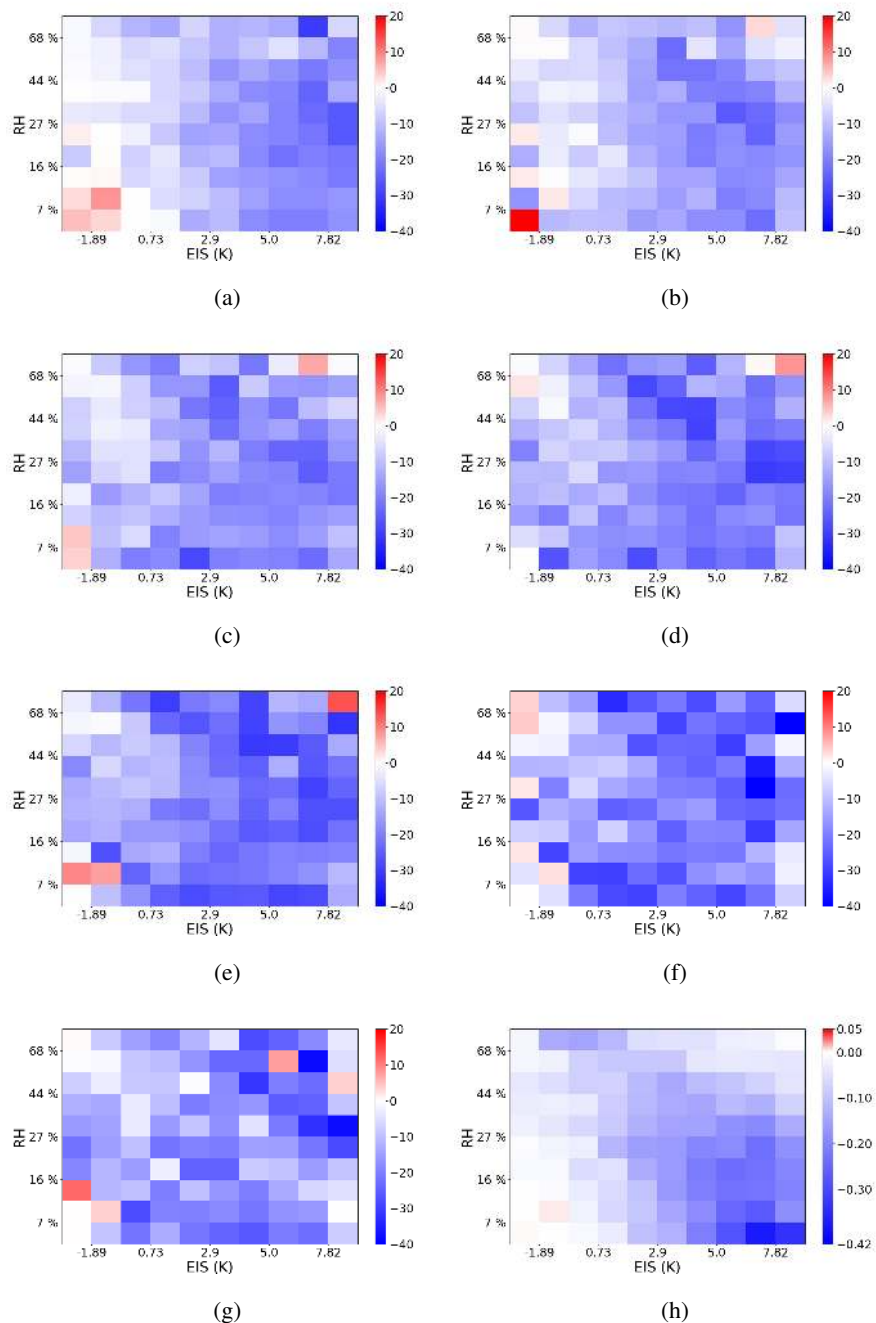


**Figure 6.** The sensitivity of CRE to aerosol ( $\lambda$ ) found with constraints on stability, RH and cloud state limits of a) .02 to .04 ( $-3.7 \frac{Wm^{-2}}{\ln(AI)}$ ), b) .04 to .06 ( $-2.2 \frac{Wm^{-2}}{\ln(AI)}$ ), c) .06 to .08 ( $-1.4 \frac{Wm^{-2}}{\ln(AI)}$ ), d) .08 to .1 ( $-1. \frac{Wm^{-2}}{\ln(AI)}$ ), e) .1 to .15 ( $-1.5 \frac{Wm^{-2}}{\ln(AI)}$ ), f) .15 to .2 ( $-5 \frac{Wm^{-2}}{\ln(AI)}$ ), and g) .2 to .4 ( $-4 \frac{Wm^{-2}}{\ln(AI)}$ )  $\frac{kg}{m^3}$ . The weighted summed sensitivity is  $-10.6 \frac{Wm^{-2}}{\ln(AI)}$ .



of CCN in the cloud leading to rapid invigoration (Christensen and Stephens, 2011). This suggests that RH may play a more pronounced role in modulating aerosol effects in thinner clouds.

The summed and weighted sensitivity with constraints on both LWP and meteorology is  $-10.6 \frac{W_m^{-2}}{\ln(AI)}$ . Overall, the largest sensitivity is seen in stable, dry environments (Figure 6h). This is due in part to their prominence, as most marine stratocumulus cloud decks occur in stable environments with a dry free troposphere from an almost continual overlying high pressure system. The smallest sensitivity occurs in unstable, dry regimes and stable, moist regimes. While these are less common, the fact that on a global scale with constraints on cloud state, some regimes show no sensitivity or a reverse Twomey effect is significant. Even with the most stringent constraints, on a global scale the reverse Twomey effect is discerned.

These results also suggest that AIE is overestimated in approaches that do not hold the LWP approximately constant. When summed and weighted by frequency of occurrence, over almost all environmental regimes, constraining LWP damps  $\lambda$  (Figure 6). The difference between the cloud regime constrained and only environmentally constrained sensitivities reveals the strong dependence of cloud response on stability, RH, and LWP. In very few unstable environments, LWP constraints act to amplify the response. This effect is only observed in the the most moist and unstable or dry, stable states that have a high density of observations. LWP constrains in these regimes pulls out otherwise obstructed or buffered signals.

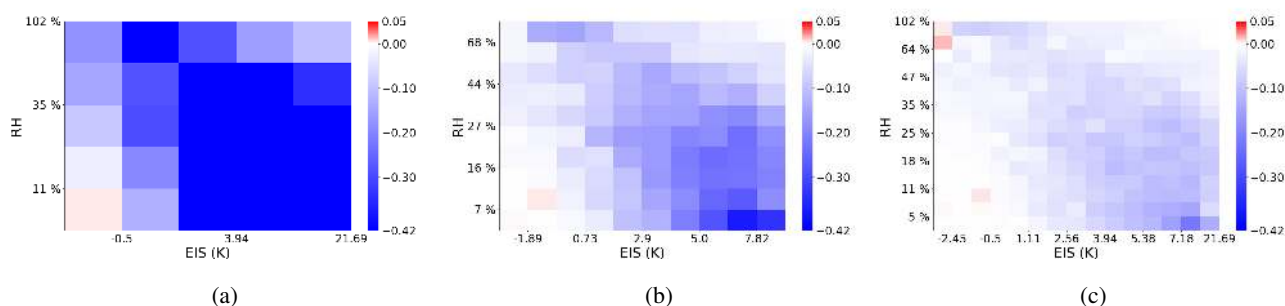


**Figure 7.** The sensitivities of CRE to aerosol from equation (4) within environmental regime resolutions of a) 5 by 5 ( $-10.8 \frac{W_m^{-2}}{\ln(AI)}$ ), b) 10 by 10 ( $-10.6 \frac{W_m^{-2}}{\ln(AI)}$ ), and c) 15 by 15 ( $-10.6 \frac{W_m^{-2}}{\ln(AI)}$ ) summed over all cloud regime states. Unlike all previous sensitivity estimates, these are weighted by occurrence.

To assess the effect of the resolution used to define environmental states when LWP constraints are added Figure 6h is replicated using 25, 100, and 225 environmental states (Figure 7). Sensitivity estimates are less varied between the three resolutions when LWP is constrained (relative to Figure 3), indicating that holding LWP fixed is essential regardless of environmental regime resolution. The inclusion of cloud regimes, however, places increasingly restrictive demands on sampling volumes since each regime must be sufficiently populated enough to allow robust sensitivities to be derived within a majority of cloud regimes.

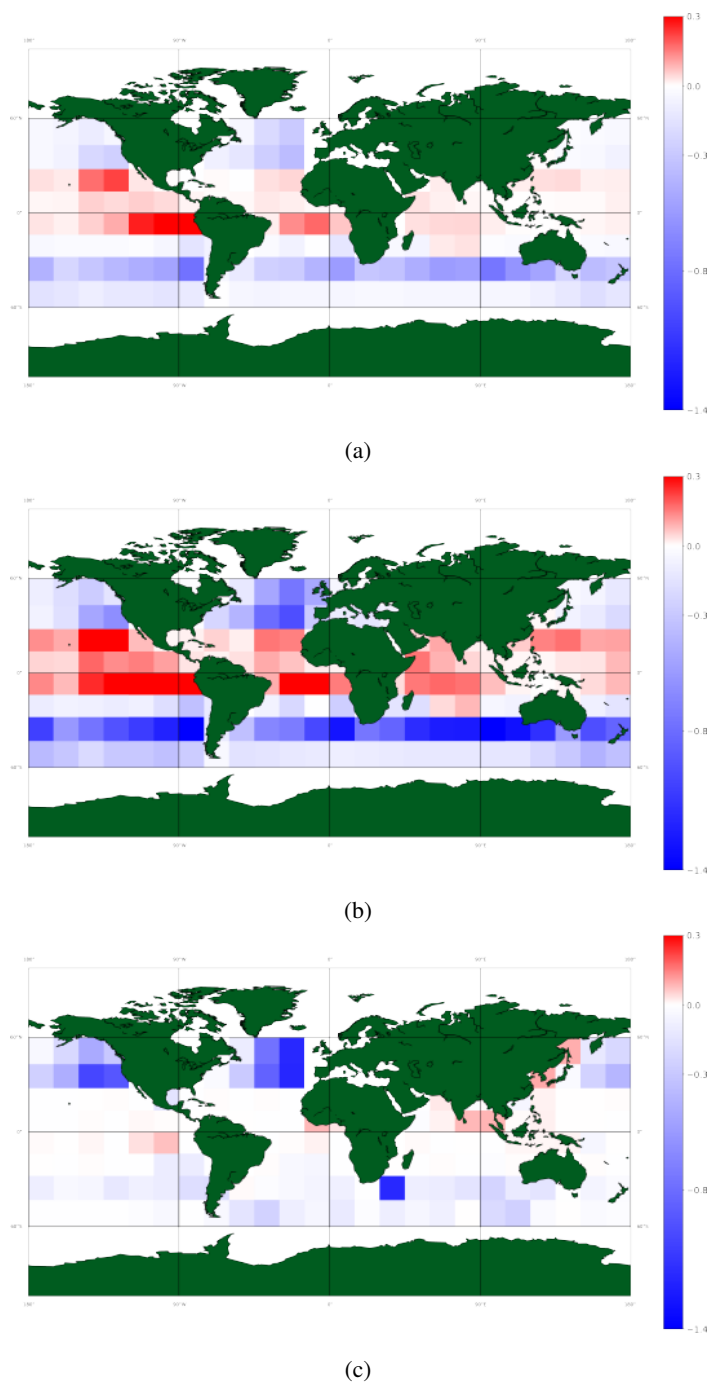


**Figure 8.** The sensitivity of CRE to aerosol ( $\lambda$ ) found with (a) no regimes constraints, (b) only cloud state constraints, and (c) only environmental constraints for each 15 by 15 region. Total sensitivities are (a) -11.8, (b) -28.5, and (c) -13.8.  $\frac{W_m^{-2}}{\ln(AI)}$ .





### 3.5 Sensitivity on Regional Scales

None of the results presented thus far have considered variability on the local scale. To account for local processes and systematic differences in aerosol (e.g. composition, size, source) not captured by the bulk, global metrics above, the cloud state and environmental regime framework is applied to all 15° grid boxes globally. Regional variations in cloud sensitivity with varying degrees of constraint on local meteorology and cloud state are shown in Figures 8 and 9. In the absence of constraints (top),  $\lambda$  exhibits larger variations in magnitude and sign than when cloud, environmental, or cloud and environmental constraints are in place (panels b and c and Figure 9). In fact, without controlling for covarying influences of stability, entrainment, and cloud morphology, vast regions of predominantly trade cumulus clouds exhibit an inverse AIE that reduce the globally integrated warm cloud AIE.

With constraints on only cloud state, the sensitivity shows greater variation in magnitude and sign than any other case (8 b). The tropics show an extreme darkening signal, much greater than the unconstrained case. The maximum cooling sensitivity occurs in the southern oceans at a much larger magnitude than the unconstrained case. These signals are likely inflated since covarying meteorological factors are not fully constrained. While limiting the effects of cloud morphology on buffering and covariance is necessary, it is not sufficient for accurately resolving global AIE.

When constrained by local meteorological conditions alone (Figure 8 c),  $\lambda$  is damped in all regions. The southern ocean no longer dominates the global AIE, instead the maximum effect is seen in the north Atlantic. The warming sensitivities, or darkening, that were prevalent in the equatorial region are significantly decreased, replaced by large regions of no  $\lambda$ , likely the result of the counteracting effect of increased entrainment and reduced particle size (Small et al., 2009).

However, clouds may be distributed among different LWP regimes, with differing sensitivities, that cumulatively cancel each other out even in similar environmental conditions. As demonstrated above, the environmental framework only controls for meteorological covariability, but cloud state plays a large role in modulating the sign and magnitude of effect. The use of only environmental regimes within a region can be appropriate when the LWP distribution is narrow but cloud morphology becomes extremely important in regions with a diverse population and broad distribution.

The inclusion of both cloud and environmental regimes limits the co-variance between aerosol, stability, cloud state, and the free atmosphere's effects on cloud radiative properties. This likely captures the true regional variation in the response of CRE to aerosol more accurately than any of the other regional estimates. When both cloud and environmental constraints are applied (Figure 9), the effect is no longer universally dampened, as was the case with only environmental regimes or enhanced as when controlling only for cloud state (Figures 8). The areas of strongest and weakest sensitivities exhibit coherent patterns that tends to align with distinct cloud and aerosol types. The largest warm cloud sensitivities are observed in the southern subtropical oceans, especially in the southeast Pacific and southern Atlantic. The California coast has a larger signal than when only regionally and environmentally constrained. The equatorial region shows a slight inverse to no effect. This is likely the region contributing to the inverse Twomey effect seen in the global regime framework for unstable, dry regions (Figure 6 h). The resulting global weighted mean AIE derived from Eqn (5) is likely more representative of the complete spectrum of global warm cloud sensitivity to aerosol than any estimates provided here or other global analyses that fail to account for local effects.

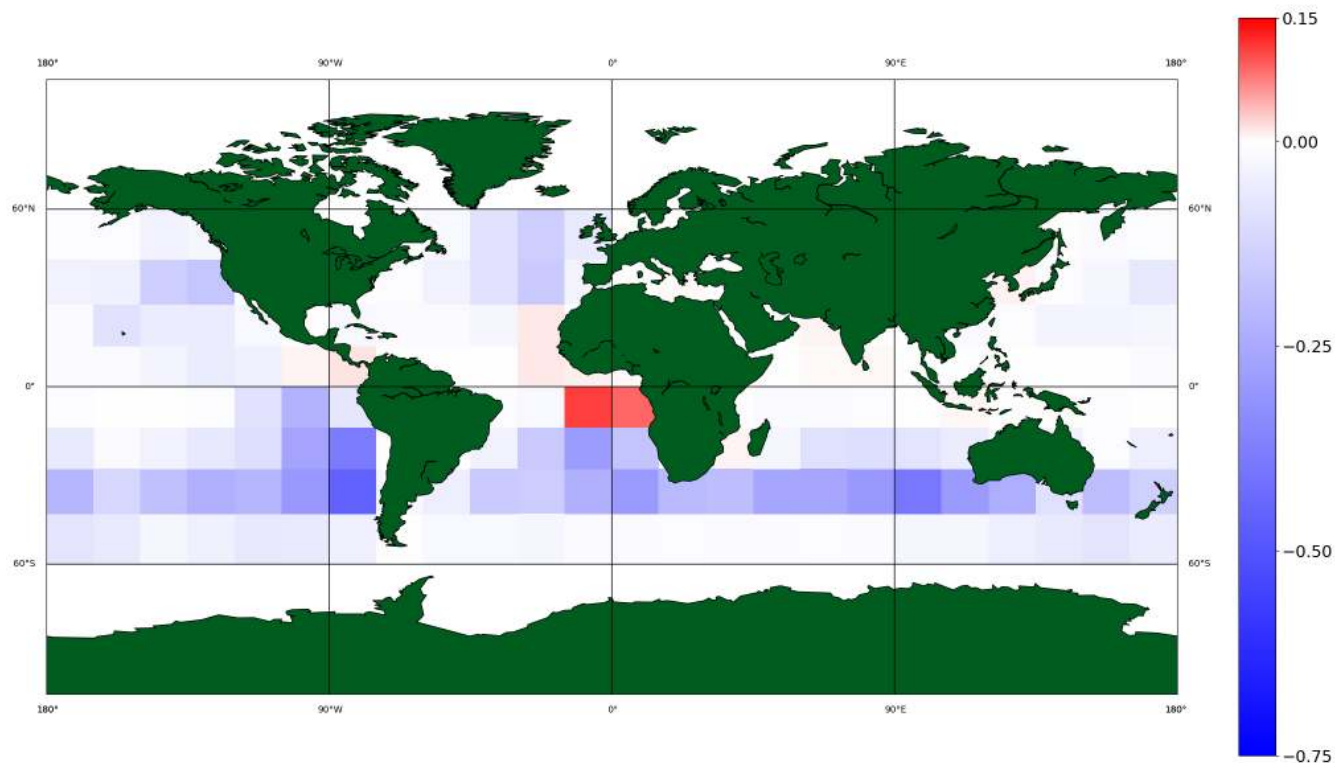


**Figure 9.** The sensitivity of CRE to aerosol ( $\lambda$ ) found on a regional basis with cloud state and environmental regime constraints. The total regime weighted, global warm cloud sensitivity to aerosol perturbations is  $-10.13 \frac{W_m^{-2}}{\ln(AI)}$ .

The inclusion of cloud state through LWP into the regime framework is vital to adhere to the original theories of Twomey (1977) and Albrecht (1989). Both assumed the LWP to be held constant, however this cannot be true of observation based estimates of the AIE unless the LWP is explicitly limited to be approximately constant. As seen in Figure 8b, limits on LWP alone are not stringent enough to elucidate the true AIE and tend to artificially enhance sensitivities. The buffering effects of the environment and local modulating factors must also be accounted for.

#### 4 Discussion

The sample regressions show in Figures 1, 2, and 3 clearly illustrate the role regimes play in constraining covarying environmental and cloud state effects on aerosol-cloud interactions. Table 1 shows that these variations translate into a range of global AIE estimates. As constraints are applied, the sensitivity decreases from -12.81 to -10.6 to  $-10.13 \frac{W_m^{-2}}{\ln(AI)}$ . The decrease in total sensitivity reveals the need to constrain LWP. Holding only cloud state constant can exacerbate the signal due to mixed meteorologies, but the first order dependence of CRE on LWP requires it to be held constant. When these are applied regionally, local signals are preserved allowing the closest to truth estimate of  $-10.13 \frac{W_m^{-2}}{\ln(AI)}$ . This estimate is only possible through the power



**Table 1.** Global radiative sensitivity estimates with varying degrees of constraints in  $\frac{\text{W m}^{-2}}{\ln(\text{AI})}$ .

No Constraints	-12.81
Cloud State Constraints	-13.12
Environmental Constraints	-11.0
Cloud & Environmental Constraints	-10.6
Cloud & Environmental Constraints Regionally	-10.13

of sampling provided by 1.8 million satellite observations partitioned among 700 regimes, or 15,200 when further partitioned on a regional basis to represent local scale processes.

In theory, partial derivatives, such as  $\frac{\partial \text{CRE}}{\partial \ln(\text{AI})}$ , assume other variables are treated as constant. The folly in treating warm clouds as only a function of aerosol is evidenced by Figures 8 and 9 where regionally  $\lambda$  changes with increasing constraints, even in the persistent and homogenous marine stratocumulus cloud deck in the southeast Pacific. Vast areas of darkening effects, that would have dramatic implications for global AIE, are substantially moderated when the local meteorology and LWP are explicitly considered (Chen et al., 2012). These regional reversals of sensitivity to aerosols demonstrate regime-specific responses even on a regional basis.

Partitioning by regime identifies environments and cloud states that buffer, amplify, or diminish cooling due to the AIE. Buffering can involve any number of processes discussed that lead to an altered response because the sensitivity is also a function of meteorological conditions (Turner et al., 2007). For example, the local meteorology, especially RH, can work to inhibit or invigorate the cloud's response to aerosol (Lu and Seinfeld, 2005; Ackerman et al., 2004). Instilling limits on RH should decrease any co-variance between the lifetime effect and RH that could arise due to RH's role in cloud cover and breakup (Kubar et al., 2015). Likewise, unstable regimes may act as a buffer to cloud brightening, evident when global observations are partitioned by EIS and RH (Figure 7).

Unstable conditions lead to strong vertical mixing and a reduced aerosol sensitivity (Cheng et al., 2017). Instability may alter the evaporation-entrainment feedback of the cloud, resulting in little to no brightening of the cloud and a severely reduced sensitivity (Jiang et al., 2006). The most unstable regimes in both figures 4 and 7 display the smallest sensitivities, which may be due to in-cloud turbulence decreasing the activation efficiency of the aerosol. Unstable regimes contain pre-convective clouds (Nishant and Sherwood, 2017). Shallow cumuli, a common pre-convective cloud type found in the equatorial trade regions, are not likely to undergo the same reaction to aerosol loading as stable warm clouds like marine stratocumulus. Environmental effects minimized by  $\lambda_{REG}$  culminate in various sensitivities seen in the bottom of Figure 8.

Without controls on the local meteorology, signals like those seen off the coast of South America, a large negative effect dominating the tropical region, may be due in part to the instability of the region and not truly reflect cloud sensitivity to aerosol loading. In the equatorial Atlantic off the coast of Africa, the strong decrease in CRE with respect to aerosol may not be the result of aerosol loading but that of surface winds decreasing cloud cover (Tubul et al., 2015). In the tropics, the warming sensitivity may be meteorologically-driven by increased frequency of trade cumuli and pre-convective clouds as



stability decreases. These positive, unconstrained sensitivities are damped with environmental regime constraints (Figure 8b and 8c), however, darkening regions still appear in the fully constrained map (Figure 9), demonstrating that although some signal in the unconstrained map is due to other influences a substantial population of warm clouds display a true, aerosol driven reverse Twomey effect.

5 The role of cloud state constraints is to hold cloud state approximately constant by constraining LWP. The distribution of warm clouds favors thin clouds, which have been shown to be more abundant and therefore more important to aerosol-cloud-radiation interactions (Hirsch et al., 2017). The results demonstrate that the sensitivity to aerosol depends strongly on LWP, consistent with Wood (2012) and Ackerman et al. (2004). This relationship between LWP and aerosol-cloud-radiation interactions must be parameterized in models in order to constrain covarying effects and models must accurately simulate  
10 LWP in order to faithfully represent the cloud response (Quaas et al., 2009; Wang et al., 2011). Model parameterizations have improved the representation of warm cloud moisture fluxes, which strongly control low cloud variance, but confidence in any AIE estimates depend on cloud parameterizations continuing to improve (Guo et al., 2014). On both global and regional scales, the environmental constraints reveal regime-specific responses (Figures 3, 8) that allow the separation of conditions that lead to a buffered response that is especially evident in the tropical regions which undergo a sign change when meteorological  
15 constrains are in place (Figure 8) (Mülmenstädt and Feingold, 2018).

The environmental and cloud regimes work to limit the co-varying effects on sensitivity estimates. This is evident when the different regime frameworks are compared (Figure 8). In the equatorial regions, controlling for the local meteorology (Figure 8c) reduces both the sensitivity and reverse Twomey effect compared to both the unconstrained (Figure 8a) and cloud state constrained (Figure 8b) estimates. In regions that exhibit strong cloud darkening effects, a deepening boundary layer,  
20 with decreasing stability, decouple warm clouds from the surface, fostering cloud break up, and in turn, decreasing the cloud fraction and associated CRE of the scene. The negative  $\lambda$  seen in the top panel of Figure 8 is likely a result of this process, which happens simultaneously with a reduced stability (Wyant et al., 1997).

Although not explicitly treated, partitioning by cloud regimes should also somewhat control for the effects of precipitation in modulating cloud sensitivity to aerosol. Clouds with less than  $150 \frac{\text{g}}{\text{m}^2}$  rarely precipitate, therefore enforcing a LWP limit at 150  
25 delineates possibly precipitating from non-precipitating clouds (L'Ecuyer et al., 2009). If precipitation does modulate aerosol-cloud interactions, these effects would be constrained in the highest LWP cloud regimes. This is not to say precipitation is not important to aerosol-cloud interactions. In principle the regime framework presented here could easily be adapted to subset scenes according to the presence of precipitation, but that is not the focus of our study.

## 5 Conclusions

30 Explicitly sorting satellite data by liquid water path, stability, and entrainment places increasingly stronger constraints on the partial derivative of CRE against  $\ln(\text{AI})$ . This is shown to limit covariance between aerosol-cloud-radiation interactions and the environment and cloud state. In the absence of such constraints, buffering or modulation of the response by local meteorology obfuscates estimates of the AIE (Stevens, 2007). By filtering abundant satellite observations according to the stability and



relative humidity of the free atmosphere and cloud liquid water path, the local meteorology and cloud morphology are held approximately constant minimizing the chance of misinterpreting covarying of meteorology and cloud morphology as aerosol effects when regressing CRE against AI (Gryspeerd et al., 2014). These environmental drivers are known to influence cloud extent and radiative effect, and with constraints through the use of regimes, we can better attribute changes in the CRE to  
5 aerosol (Turner et al., 2007). Our results suggest that without constraints, the global mean AIE can be over-estimated by as much as 40% and regional variations can be artificially enhanced by as much as a factor of 2.

With environmental and cloud regime constraints in place on a regional basis, strong, regionally specific cloud responses can be identified that can confidently be attributed to aerosols. Clouds in the southern subtropical oceans exhibit the largest sensitivity to aerosol reflecting the interactions between the marine stratocumulus decks in the southeast Pacific and south  
10 Atlantic, which interact with aerosol. Trade cumuli in the equatorial region show a much smaller, almost negligible signal comparatively. In the northern oceans, warm cloud decks from mid-latitude cyclones through the north Atlantic interact with North American and European emissions, leading to a cooling effect.

Interestingly even after cloud state and meteorology are controlled, the analysis still reveals coherent regions of aerosol forced cloud darkening effect (Figures 6h, 9). This aggregate dimming, or reverse Twomey, effect occurs in 15% of the regions  
15 studied and appears to be a robust characteristic of low LWP clouds in unstable, dry environments. This is similar to other observation based studies which found the same dimming effect in  $\sim 20\%$  of warm clouds (Chen et al., 2012). Our study suggests such clouds are sufficiently abundant to consistently yield a net inverse sensitivity over a substantial, coherent, region of the globe. Models must be able to recreate warm cloud responses, including the reverse Twomey effect, if they are to accurately simulate global aerosol indirect effects.

Both on a regional and global scale, constraints reduce co-variance of sensitivity estimates (Gryspeerd and Stier, 2012). With  
20 constraints, the sensitivity can range from .46 to  $-.11 \frac{Wm^{-2}}{\ln(AI)}$  on a regional scale, while without constraints the range increases from .77 to  $-.52 \frac{Wm^{-2}}{\ln(AI)}$ , signaling covarying influences and buffering by the cloud distort the signal even on a regional scale. Future regime classifications should prescribe precipitation limits to further separate the effects of aerosol-cloud-precipitation interactions, which are especially important to the cloud lifetime effect, where precipitation suppression leads to a larger cloud  
25 extent and lifetime.

*Data availability.* All satellite observations and MERRA-2 reanalysis used in this study are available for download through the NASA's Data Portal at <http://doi.org/10.17616/R3106C>.

*Competing interests.* The authors declare that they have no conflict of interest.



*Acknowledgements.* This work was supported by CloudSat/CALIPSO Science Team grant #NNX13AQ32G. All data used in this study were obtained through the CloudSat Data Processing Center at <http://www.cloudsat.cira.colostate.edu/>.



## References

- Ackerman, A. S., Kirkpatrick, M. P., Stevens, D. E., and Toon, O. B.: The impact of humidity above stratiform clouds on indirect aerosol climate forcing, *Nature*, 432, 1014, 2004.
- Ångström, A.: On the atmospheric transmission of sun radiation and on dust in the air, *Geografiska Annaler*, 11, 156–166, 1929.
- 5 Austin, R. T., Heymsfield, A. J., and Stephens, G. L.: Retrieval of ice cloud microphysical parameters using the CloudSat millimeter-wave radar and temperature, *Journal of Geophysical Research: Atmospheres*, 114, 2009.
- Bony, S. and Dufresne, J.-L.: Marine boundary layer clouds at the heart of tropical cloud feedback uncertainties in climate models, *Geophysical Research Letters*, 32, 2005.
- Boucher, O., Randall, D., Artaxo, P., Bretherton, C., Feingold, G., Forster, P., Kerminen, V.-M., Kondo, Y., Liao, H., Lohmann, U., et al.:  
10 Clouds and aerosols, in: *Climate change 2013: the physical science basis. Contribution of Working Group I to the Fifth Assessment Report of the Intergovernmental Panel on Climate Change*, pp. 571–657, Cambridge University Press, 2013.
- Bretherton, C., Blossey, P. N., and Uchida, J.: Cloud droplet sedimentation, entrainment efficiency, and subtropical stratocumulus albedo, *Geophysical research letters*, 34, 2007.
- Chen, Y.-C., Christensen, M., Xue, L., Sorooshian, A., Stephens, G., Rasmussen, R., and Seinfeld, J.: Occurrence of lower cloud albedo  
15 in ship tracks, *Atmospheric Chemistry and Physics*, 12, 8223–8235, 2012.
- Chen, Y.-C., Christensen, M. W., Stephens, G. L., and Seinfeld, J. H.: Satellite-based estimate of global aerosol–cloud radiative forcing by marine warm clouds, *Nature Geoscience*, 7, 643, 2014.
- Cheng, F., Zhang, J., He, J., Zha, Y., Li, Q., and Li, Y.: Analysis of aerosol-cloud-precipitation interactions based on MODIS data, *Advances in Space Research*, 59, 63–73, 2017.
- 20 Christensen, M. W. and Stephens, G. L.: Microphysical and macrophysical responses of marine stratocumulus polluted by underlying ships: Evidence of cloud deepening, *Journal of Geophysical Research: Atmospheres*, 116, 2011.
- Dagan, G., Koren, I., Altaratz, O., and Heiblum, R. H.: Time-dependent, non-monotonic response of warm convective cloud fields to changes in aerosol loading, *Atmospheric Chemistry and Physics*, 17, 7435–7444, 2017.
- Fan, J., Wang, Y., Rosenfeld, D., and Liu, X.: Review of aerosol–cloud interactions: Mechanisms, significance, and challenges, *Journal of  
25 the Atmospheric Sciences*, 73, 4221–4252, 2016.
- Feingold, G.: Modeling of the first indirect effect: Analysis of measurement requirements, *Geophysical research letters*, 30, 2003.
- Feingold, G. and Kreidenweis, S. M.: Cloud processing of aerosol as modeled by a large eddy simulation with coupled microphysics and aqueous chemistry, *Journal of Geophysical Research: Atmospheres*, 107, AAC–6, 2002.
- Ghan, S., Wang, M., Zhang, S., Ferrachat, S., Gettelman, A., Griesfeller, J., Kipling, Z., Lohmann, U., Morrison, H., Neubauer, D.,  
30 et al.: Challenges in constraining anthropogenic aerosol effects on cloud radiative forcing using present-day spatiotemporal variability, *Proceedings of the National Academy of Sciences*, 113, 5804–5811, 2016.
- Grandey, B. and Stier, P.: A critical look at spatial scale choices in satellite-based aerosol indirect effect studies, *Atmospheric Chemistry and Physics*, 10, 11 459–11 470, 2010.
- Greenwald, T. J., L'Ecuyer, T. S., and Christopher, S. A.: Evaluating specific error characteristics of microwave-derived cloud liquid water  
35 products, *Geophysical Research Letters*, 34, 2007.
- Gryspeerd, E. and Stier, P.: Regime-based analysis of aerosol-cloud interactions, *Geophysical Research Letters*, 39, 2012.





- Gryspeerd, E., Stier, P., and Partridge, D.: Satellite observations of cloud regime development: the role of aerosol processes, *Atmospheric Chemistry and Physics*, 14, 1141–1158, 2014.
- Gryspeerd, E., Quaas, J., and Bellouin, N.: Constraining the aerosol influence on cloud fraction, *Journal of Geophysical Research: Atmospheres*, 121, 3566–3583, 2016.
- 5 Guo, Z., Wang, M., Qian, Y., Larson, V. E., Ghan, S., Ovchinnikov, M., Bogenschütz, P. A., Zhao, C., Lin, G., and Zhou, T.: A sensitivity analysis of cloud properties to CLUBB parameters in the single-column Community Atmosphere Model (SCAM5), *Journal of Advances in Modeling Earth Systems*, 6, 829–858, 2014.
- Hahn, C. and Warren, S.: A Gridded Climatology of Clouds over Land (1971-96) and Ocean (1954-97 from Surface Observations Worldwide, Tech. rep., Office of Biological and Environmental Research, 2007.
- 10 Hirsch, E., Koren, I., Altaratz, O., Levin, Z., and Agassi, E.: Enhanced humidity pockets originating in the mid boundary layer as a mechanism of cloud formation below the lifting condensation level, *Environmental Research Letters*, 12, 024020, 2017.
- Jiang, H., Xue, H., Teller, A., Feingold, G., and Levin, Z.: Aerosol effects on the lifetime of shallow cumulus, *Geophysical Research Letters*, 33, 2006.
- Juárez, T., Kahn, B., Fetzer, E., et al.: Cloud-type dependencies of MODIS and AMSR-E liquid water path differences, *Atmospheric Chemistry and Physics Discussions*, 9, 3367–3399, 2009.
- 15 Köhler, H.: The nucleus in and the growth of hygroscopic droplets, *Transactions of the Faraday Society*, 32, 1152–1161, 1936.
- Kubar, T. L., Stephens, G. L., Lebsock, M., Larson, V. E., and Bogenschütz, P. A.: Regional assessments of low clouds against large-scale stability in CAM5 and CAM-CLUBB using MODIS and ERA-Interim reanalysis data, *Journal of Climate*, 28, 1685–1706, 2015.
- L’Ecuyer, T. S. and Jiang, J. H.: Touring the atmosphere aboard the A-Train, in: *AIP Conference Proceedings*, vol. 1401, pp. 245–256, 20  
AIP, 2011.
- L’Ecuyer, T. S., Berg, W., Haynes, J., Lebsock, M., and Takemura, T.: Global observations of aerosol impacts on precipitation occurrence in warm maritime clouds, *Journal of Geophysical Research: Atmospheres*, 114, 2009.
- Lee, S. S., Penner, J. E., and Saleeby, S. M.: Aerosol effects on liquid-water path of thin stratocumulus clouds, *Journal of Geophysical Research: Atmospheres*, 114, 2009.
- 25 Lee, S.-S., Feingold, G., and Chuang, P. Y.: Effect of aerosol on cloud–environment interactions in trade cumulus, *Journal of the Atmospheric Sciences*, 69, 3607–3632, 2012.
- Levy, R., Remer, L., Kleidman, R., Mattoo, S., Ichoku, C., Kahn, R., and Eck, T.: Global evaluation of the Collection 5 MODIS dark-target aerosol products over land, *Atmospheric Chemistry and Physics*, 10, 10399–10420, 2010.
- Liu, J., Li, Z., and Cribb, M.: Response of Marine Boundary Layer Cloud Properties to Aerosol Perturbations Associated with Meteorological Conditions from the 19-Month AMF-Azores Campaign, *Journal of the Atmospheric Sciences*, 73, 4253–4268, 2016.
- 30 Lohmann, U. and Feichter, J.: Global indirect aerosol effects: a review, *Atmospheric Chemistry and Physics*, 5, 715–737, 2005.
- Lohmann, U. and Lesins, G.: Stronger constraints on the anthropogenic indirect aerosol effect, *Science*, 298, 1012–1015, 2002.
- Lu, M.-L. and Seinfeld, J. H.: Study of the aerosol indirect effect by large-eddy simulation of marine stratocumulus, *Journal of the atmospheric sciences*, 62, 3909–3932, 2005.
- 35 Mülmstädt, J. and Feingold, G.: The Radiative Forcing of Aerosol–Cloud Interactions in Liquid Clouds: Wrestling and Embracing Uncertainty, *Current Climate Change Reports*, 4, 23–40, 2018.
- Nam, C., Bony, S., Dufresne, J.-L., and Chepfer, H.: The ‘too few, too bright’ tropical low-cloud problem in CMIP5 models, *Geophysical Research Letters*, 39, 2012.



- Nishant, N. and Sherwood, S.: A Cloud-Resolving Model Study of Aerosol-Cloud Correlation in a Pristine Maritime Environment, *Geophysical Research Letters*, 2017.
- Oke, T. R.: *Boundary layer climates*, Routledge, 2002.
- Oreopoulos, L., Cho, N., Lee, D., and Kato, S.: Radiative effects of global MODIS cloud regimes, *Journal of Geophysical Research: Atmospheres*, 121, 2299–2317, 2016.
- 5 Penner, J. E., Andreae, M., Annegarn, H., Barrie, L., Feichter, J., Hegg, D., Jayaraman, A., Leaitch, R., Murphy, D., Nganga, J., et al.: Aerosols, their direct and indirect effects, in: *Climate Change 2001: The Scientific Basis. Contribution of Working Group I to the Third Assessment Report of the Intergovernmental Panel on Climate Change*, pp. 289–348, Cambridge University Press, 2001.
- Platnick, S. and Twomey, S.: Determining the susceptibility of cloud albedo to changes in droplet concentration with the Advanced Very  
10 High Resolution Radiometer, *Journal of Applied Meteorology*, 33, 334–347, 1994.
- Quaas, J., Ming, Y., Menon, S., Takemura, T., Wang, M., Penner, J. E., Gettelman, A., Lohmann, U., Bellouin, N., Boucher, O., et al.: Aerosol indirect effects—general circulation model intercomparison and evaluation with satellite data, *Atmospheric Chemistry and Physics*, 9, 8697–8717, 2009.
- Remer, L. A., Kaufman, Y., Tanré, D., Mattoo, S., Chu, D., Martins, J. V., Li, R.-R., Ichoku, C., Levy, R., Kleidman, R., et al.: The MODIS  
15 aerosol algorithm, products, and validation, *Journal of the atmospheric sciences*, 62, 947–973, 2005.
- Sassen, K., Wang, Z., and Liu, D.: Global distribution of cirrus clouds from CloudSat/Cloud-Aerosol lidar and infrared pathfinder satellite observations (CALIPSO) measurements, *Journal of Geophysical Research: Atmospheres*, 113, 2008.
- Small, J. D., Chuang, P. Y., Feingold, G., and Jiang, H.: Can aerosol decrease cloud lifetime?, *Geophysical Research Letters*, 36, 2009.
- Sorooshian, A., Feingold, G., Lebsock, M. D., Jiang, H., and Stephens, G. L.: On the precipitation susceptibility of clouds to aerosol  
20 perturbations, *Geophysical Research Letters*, 36, 2009.
- Stephens, G.: Radiation profiles in extended water clouds. I: Theory, *Journal of the Atmospheric Sciences*, 35, 2111–2122, 1978.
- Stephens, G. L.: Cloud feedbacks in the climate system: A critical review, *Journal of climate*, 18, 237–273, 2005.
- Stevens, B.: On the growth of layers of nonprecipitating cumulus convection, *Journal of the atmospheric sciences*, 64, 2916–2931, 2007.
- Stevens, B. and Feingold, G.: Untangling aerosol effects on clouds and precipitation in a buffered system, *Nature*, 461, 607–613, 2009.
- 25 Stier, P.: Limitations of passive remote sensing to constrain global cloud condensation nuclei, 2016.
- Su, W., Loeb, N. G., Xu, K.-M., Schuster, G. L., and Eitzen, Z. A.: An estimate of aerosol indirect effect from satellite measurements with concurrent meteorological analysis, *Journal of Geophysical Research: Atmospheres*, 115, 2010.
- Tsushima, Y., Ringer, M. A., Koshiro, T., Kawai, H., Roehrig, R., Cole, J., Watanabe, M., Yokohata, T., Bodas-Salcedo, A., Williams, K. D., et al.: Robustness, uncertainties, and emergent constraints in the radiative responses of stratocumulus cloud regimes to future  
30 warming, *Climate dynamics*, 46, 3025–3039, 2016.
- Tubul, Y., Koren, I., and Altaratz, O.: The tropical Atlantic surface wind divergence belt and its effect on clouds, *Earth System Dynamics*, 6, 781, 2015.
- Turner, D. D., Vogelmann, A., Austin, R. T., Barnard, J. C., Cady-Pereira, K., Chiu, J. C., Clough, S. A., Flynn, C., Khaiyer, M. M., Liljegren, J., et al.: Thin liquid water clouds: Their importance and our challenge, *Bulletin of the American Meteorological Society*, 88,  
35 177–190, 2007.
- Van der Dussen, J., De Roode, S., Gesso, S. D., and Siebesma, A.: An LES model study of the influence of the free tropospheric thermodynamic conditions on the stratocumulus response to a climate perturbation, *Journal of Advances in Modeling Earth Systems*, 7, 670–691, 2015.



- Wang, M., Ghan, S., Ovchinnikov, M., Liu, X., Easter, R., Kassianov, E., Qian, Y., and Morrison, H.: Aerosol indirect effects in a multi-scale aerosol-climate model PNNL-MMF, *Atmospheric Chemistry and Physics*, 11, 5431, 2011.
- Wentz, F. J. and Meissner, T.: Supplement 1 algorithm theoretical basis document for AMSR-E ocean algorithms, NASA: Santa Rosa, CA, USA, 2007.
- 5 Williams, K. and Webb, M.: A quantitative performance assessment of cloud regimes in climate models, *Climate dynamics*, 33, 141–157, 2009.
- Wood, R.: Stratocumulus clouds, *Monthly Weather Review*, 140, 2373–2423, 2012.
- Wood, R. and Bretherton, C. S.: Boundary layer depth, entrainment, and decoupling in the cloud-capped subtropical and tropical marine boundary layer, *Journal of climate*, 17, 3576–3588, 2004.
- 10 Wood, R. and Bretherton, C. S.: On the relationship between stratiform low cloud cover and lower-tropospheric stability, *Journal of climate*, 19, 6425–6432, 2006.
- Wood, R., Jensen, M. P., Wang, J., Bretherton, C. S., Burrows, S. M., Del Genio, A. D., Fridlind, A. M., Ghan, S. J., Ghate, V. P., Kollias, P., et al.: Planning the next decade of coordinated research to better understand and simulate marine low clouds, *Bulletin of the American Meteorological Society*, 97, 1699–1702, 2016.
- 15 Wood, R., O, K.-T., Bretherton, C. S., Mohrmann, J., Albrecht, B. A., Zuidema, P., Ghate, V., Schwartz, C., Eloranta, E., Glienke, S., et al.: Ultraclean Layers and Optically Thin Clouds in the Stratocumulus-to-Cumulus Transition. Part I: Observations, *Journal of the Atmospheric Sciences*, 75, 1631–1652, 2018.
- Wyant, M. C., Bretherton, C. S., Rand, H. A., and Stevens, D. E.: Numerical simulations and a conceptual model of the stratocumulus to trade cumulus transition, *Journal of the atmospheric sciences*, 54, 168–192, 1997.